Marie Skłodowska-Curie (MSCA) – Innovative Training Networks (ITN)
H2020-MSCA-ITN European Training Networks

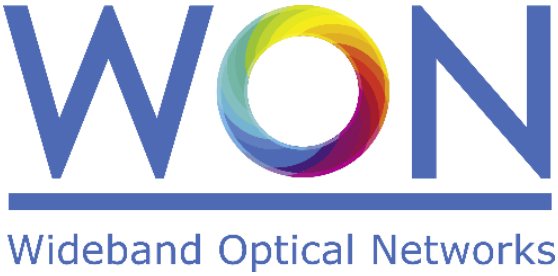

Wideband Optical Networks [WON]

Grant agreement ID: 814276

WP1 – Network management: planning and control

Deliverable D1.2 Physical layer aware networking in multi-optical band systems

This project has received funding from the European Union's Horizon 2020 research and innovation programme under the Marie Skłodowska-Curie grant agreement 814276.

Document Details

Work Package	WP1 – Network management: planning and control
Deliverable number	D1.2
Deliverable Title	Physical layer aware networking in multi-optical band systems
Lead Beneficiary:	DTU
Deliverable due date:	31 December 2021
Actual delivery date:	1 February 2022
Dissemination level:	Public

Project Details

Project Acronym	WON
Project Title	Wideband Optical Networks
Call Identifier	H2020-MSCA-2018 Innovative Training Networks
Coordinated by	Aston University, UK
Start of the Project	1 January 2019
Project Duration	48 months
WON website:	https://won.astonphotonics.uk/
CORDIS Link	https://cordis.europa.eu/project/rcn/218205/en

WON Consortium and Acronyms

Consortium member	**Legal Entity Short Name**
Aston University	Aston
Danmarks Tekniske Universitet	DTU
VPIphotonics GmbH	VPI
Infinera Portugal	INF PT
Fraunhofer HHI	HHI
Politecnico di Torino	POLITO
Technische Universiteit Eidhoven	TUE
Universiteit Gent	UG
Keysight Technologies	Keysight
Finisar Germany GmbH	Finisar
Orange SA	Orange
Technische Universitaet Berlin	TUB
Instituto Superior Tecnico, University of Lisboa	IST

Abbreviations

ASE:	Amplified Spontaneous Emission
CA:	Consortium Agreement
CUT:	Channel Under Test
EDFA:	Erbium-Doped Fiber Amplifier
FF:	First-Fit
FWM:	Four Wave Mixing
GA:	Grant Agreement
GN:	Gaussian Noise
GSNR:	Generalized Signal-to-Noise Ratio
JPDF:	Joint Probability Density Function
LP:	Light-path
NLI:	Nonlinear Interference
NLPN:	Nonlinear Phase Noise
OLA:	Optical Line Amplifier
OLS:	Optical Line System
OSNR:	Optical Signal to Noise Ratio
PM:	Polarization Maintaining
P&P:	Pump-and-Probe
PSD:	Power Spectral Density
QAM:	Quadrature Amplitude Modulation
QPSK:	Quadrature Phase Shift Keying
QoT:	Quality of Transmission
ROADM	Re-configurable optical add-drop multiplexer
RWA:	Routing and Wavelength Assignment
SNAP:	Statistical Network Assessment Process
SNR:	Signal to Noise Ratio
SRS:	Stimulated Raman Scattering
SSFM:	Split-Step Fourier Method
SSMF:	Standard Single Mode Fiber
SPM:	Self-Phase Modulation
XPM:	Cross-Phase Modulation
TDFA:	Thulium-doped Fiber Amplifier
WDM:	Wavelength-Division Multiplexed

CONTENT

LIST OF FIGURES

LIST OF TABLES

EXECUTIVE SUMMARY

The present scientific deliverable is part of Work Package 1 “Network management: planning and control”, in turn part of the ETN project WON “Wideband Optical Networks”, funded under the Horizon 2020 Marie Skłodowska-Curie scheme Grant Agreement 814276.

This document provides details on the derivation and simulative assessment of a spatially and spectrally disaggregated model for NLI generation within optical networks. The main topics carried out and presented in this text are: (i) the observation of spatially separated cross-phase modulation generation in a wide variety of 400G ZR+ 64 GBd pump-and-probe simulations, and the existence of a per-span upper bound that depends solely upon accumulated dispersion. (ii) An optimal strategy for C+L multi-band power control assessing and the demonstration that the L-band can be optimized independently. (iii) C+L+S optical power optimization where band division multiplexing (BDM) enables a network traffic increase which is slightly less than but comparable to the spatial division multiplexing (SDM) scenario, without requiring additional fiber cables.

1. Overview of NLI Generation in Wideband Optical Networks

The current increase in internet data traffic [1] motivates a search for technologies that maximize available telecommunications infrastructures and provide a greater degree of efficiency, both with respect to spectral occupation and economic expenditure. Wideband optical network implementations provide an attractive solution, satisfying these requirements by utilizing wavelengths lying outside of the C-band within already-deployed optical fiber. Furthermore, to achieve wideband upgrades and higher degrees of flexibility, a disaggregated approach is envisaged, where signals are transmitted across independent lightpaths in a multi-vendor scenario. This creates a dynamic environment where it is important to develop a benchmark to assess the system characteristics even when information from third parties is not available.

Assessing nonlinear interference (NLI) in an aggregated manner can be performed quickly and with high accuracy closed-form implementations of the Gaussian noise (GN) model, however in a disaggregated network scenario spectral and device information may not be fully available to all parties, along with the presence of alien wavelengths, both of which severely hamper an aggregated NLI modelling approach. An alternative scenario is to perform the NLI modelling from a disaggregated point of view, with all channels being treated separately.

In this approach, a conventional manner of describing the quality of the signal transmitted is by use of the general signal-to-noise ratio (GSNR) which for the *i*th channel under test (CUT) within a spectral comb comprised of *n* channels is described by **Error! Reference source not found.**

$$\mathrm{GSNR}_i^{-1} = \mathrm{OSNR}_i^{-1} + \mathrm{SNR}_{NL,i}^{-1},$$

where the optical SNR $\mathrm{OSNR}_i = {P_{s,i}}/{P_{ASE}}$ represents the contribution from the amplifiers in the link due to the amplified spontaneous emission (ASE) noise, while the $\mathrm{SNL}_{NL,i} = {P_{s,i}}/{P_{NLI,i}}$ quantifies the NLI generated during propagation through the fiber spans. $P_{s,i}$ is the signal input power in the *i*th channel, P_{ASE} is ASE noise, and $P_{NLI,i}$ the accumulated NLI along with propagation in channel *i*th. In general, the NLI is composed of the self-phase modulation (SPM), cross-phase modulation (XPM), with other four-wave mixing (FWM) effects being negligible for most conventional transmission scenarios.

Considering spectral disaggregation, the NLI generated for a specific CUT in an arbitrary spectral configuration, P_{NLI}, can be expressed as the sum of individual contributions for each channel *i* as in

$$P_{NLI} = P_{NLI,0} + \sum_{i \neq 0} P_{NLI,i},$$

in which $P_{NLI,0}$ accounts for the SPM and $P_{NLI,i}$ for the XPM. When both spatial and spectral disaggregation is achieved, the NLI may be summed on a span-by-span and channel-by-channel basis. In this way, the nonlinear SNR contribution of each channel is calculated as

$$\mathrm{SNR_{NL}} = \left[\sum_{n=1}^{N_s}\left(\frac{1}{\mathrm{SNR_{NL,n,0}}} + \sum_{i \neq 0}\frac{1}{\mathrm{SNR_{NL,n,i}}}\right)\right]^{-1},$$

where N_s is the total number of spans.

2. Cross-channel NLI generation in disaggregated optical line systems

To investigate the generation of XPM in a disaggregated approach, a pump-and-probe (P&P) scenario is explored, considering multiple values of accumulated dispersion through a split-step Fourier method (SSFM) simulation campaign. Two channels are considered, located at 194.05 THz and 193.9 THz, representing the interfering channel and the CUT, respectively. The CUT is operated at -20 dBm to avoid the generation of SPM, whereas the pump is set to 6 dBm to ensure that a considerable amount of NLI is generated. Both channels are root-raised cosine shaped with 0.15 roll-off factor and a 64 Gbaud symbol rate. A polarization-multiplexed (PM) - quadrature phase shift keying (QPSK) signal is transmitted over the CUT, while a PM-QPSK and PM-16-quadrature amplitude modulation (QAM) signal is transmitted over the pump. The use of two different modulation formats over the pump creates a scenario where modulation format dependence may be studied. For comparison, two system configurations are considered: (i) propagation through a 40-span periodic optical line system (OLS), operated in transparency, and considering ideal Erbium-doped fiber amplifiers (EDFA)s. (ii) signals transmitted over a single fiber span 40 separated times, with predistortion applied to the pump and the probe equal to the dispersion accumulated by the transmission through the *n* preceding spans. For both cases, the following characteristics are considered: constant loss coefficient $\alpha_{dB} = 0.2\,\mathrm{dB/km}$, nonlinear coefficient $\gamma = 1.27\,\frac{1}{\mathrm{W}}/\mathrm{km}$, dispersion coefficients $D = [4, 8, 16]\ \mathrm{ps/(nm \cdot km)}$, and fiber length $L_s = [50, 80, 100, 200]\ \mathrm{km}$. The signal at the end of each span passes through an ideal receiver which contains a dispersion compensation stage, followed by a matched filter, and recovering only the average (constant) phase. The accumulated NLI power is obtained by calculating the $\mathrm{SNR_{NL}}$ upon the received constellation.

The results for the periodic and single-span simulation scenarios are presented in Fig. 1a and Fig. 1b, for a QPSK and 16-QAM modulated pump and considering D= 16 ps/(nm ·km) line scenario, for several fiber lengths. The gradient of the NLI efficiency, $\Delta\eta$, is considered where η corresponds to the NLI power normalized over $\mathrm{P_{CUT}^2 P_{ch}}$. For all scenarios, $\Delta\eta$ is span length-dependent and a similar result is achieved for all span lengths for the Gaussian modulated pump scenario. Moreover, all single-span simulations tend towards an identical asymptote that corresponds to the level given by the Gaussian modulated pump transmission. Additionally, as a conservative estimation of the single-span asymptote, the amount of NLI generated using a GN model implementation is included in Fig. 1. In comparison, the periodic and single-span models demonstrate a large transient which is not present in the GN model/Gaussian modulation scenarios.

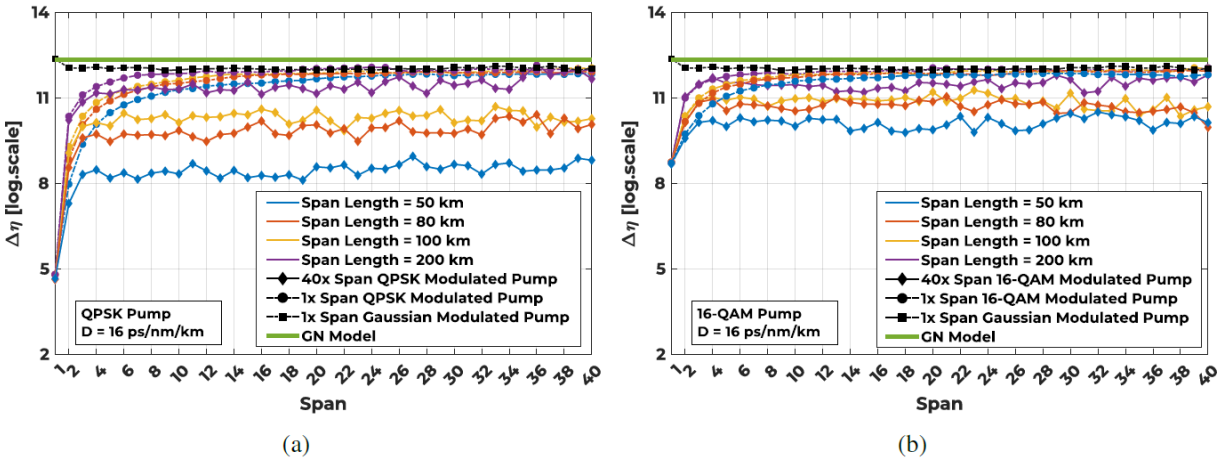

Figure 1: NLI efficiency gradient vs. the number of spans for (a) QPSK and (b) 16-QAM. The solid curves are the periodic line simulations. Dashed curves are the corresponding single-span results, with coloured circles for a QPSK/16-QAM modulated pump and black squares for a Gaussian modulated pump. The green lines are the levels given by the GN model.

To highlight the use of the GN model as a conservative upper bound, in Fig.2 the asymptotic $\Delta\eta$ is presented for a selection of line configurations. The metric is calculated by finding the average $\Delta\eta$ over the last 20 spans of propagation. A difference of at least 2 dB is shown in some cases, with this discrepancy decreasing for larger fiber lengths. It is important to note that if the dispersion of the channel is available, the use of a disaggregated model provides an increase in the accuracy of the NLI prediction, reducing this worst-case 2 dB value. In Fig. 2b, the NLI accumulation in mixed fiber scenarios is presented by considering an OLS consisting of 20 fiber spans with D= 4 ps/(nm· km) followed by 20 fiber spans with D=16 ps/(nm· km), and vice versa. The change in the dispersion induces a transient and the $\Delta\eta$ tends towards a stable value after this. The spatial disaggregation of the XPM is valid even for non-periodic OLS as shown in Fig. 2a. Moreover, the GN model upper bound also accommodates these transient as highlighted in Fig. 2a.

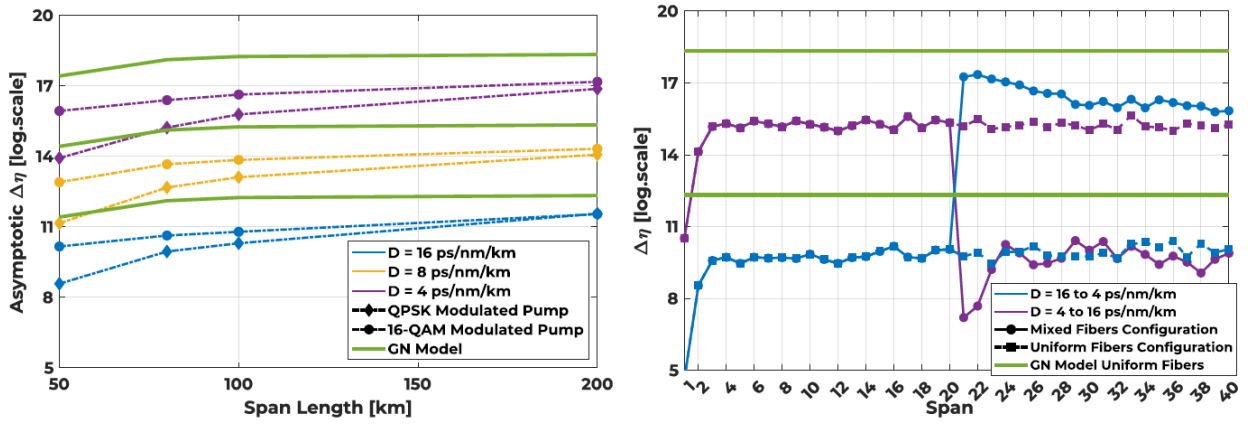

Figure 2: (a) periodic simulation campaign vs. span length, averaging the results of the last 20 spans, for QPSK and 16-QAM modulation formats. (b) mixed fiber configurations along with levels that correspond to 40 uniform spans of each fiber dispersion. In both plots the green lines are the levels given by the GN model.

To conclude this section, when working within a wideband and/or disaggregated optical network scenario, it is essential to be able to quantify the QoT impairments that arise because of unknown transmission parameters, and to be able to approach NLI generation from a spectrally and spatially separated perspective. We have demonstrated that channels

transmitted across a lightpath with partially or fully unknown history have a similarly unknown impact upon the NLI generation, which can be understood as an unknown amount of previously accumulated dispersion. Thus, it is possible to use an infinitely predistorted signal model that represents a Gaussian channel and corresponds to the GN model implementation to maximally quantify this uncertainty, which may then be improved depending upon knowledge of the lightpath history. We furthermore show that this approach remains valid even when non-periodic links are considered, as would be expected within a realistic disaggregated network segment.

3. Single and Multi-Band Optimized Power Control

For the vast majority of present optical networks, the C-band is by far the most commonly used for transmission, but state-of-art research has shown that extending transmission first into the L-band is a cost-effective capacity upgrade that utilizes the current network infrastructure with a relatively small penalty in average network traffic in comparison with fiber doubling solutions [2]. In this scenario (C+L band), it is necessary to add transceivers and optical line amplifiers (OLA) to cover both bands. Moreover, stimulated Raman scattering (SRS) becomes significant, as it causes a power transfer from higher to lower frequencies, which subsequently changes NLI generation. This power transfer makes the problem of power control optimization complex if the goal is to maintain a desired quality of transmission (QoT) in already-operational C-band systems. To assess the power control optimization, the setup in Fig. 3a is considered in which a power control unit defines the operation points for the C- and L-band amplifiers. The optimum operation point launch power is defined using an optimization algorithm based on a QoT estimator.

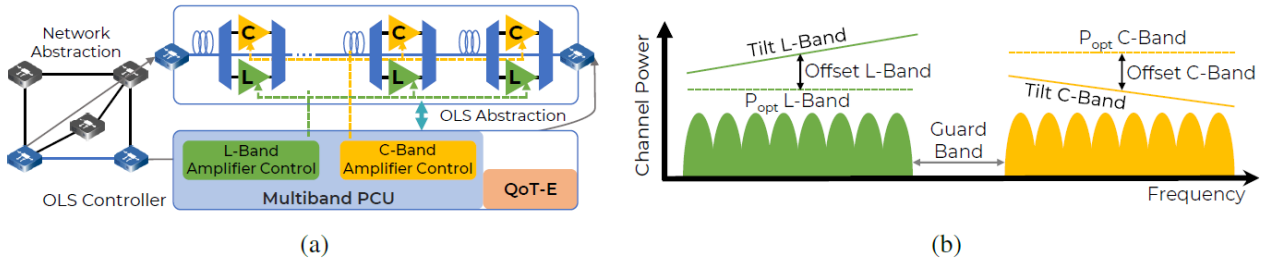

Figure 3: (a) Network and OLS representation of C+L transmission. The C- and L-bands are amplified by separate OLAs. The OLS controller implements a QoT-E module that calculates a (sub-) optimum power profile set by the PCU. (b) Representation of spectral load in C+L systems, with launch power offset and tilt used to compensate for SRS.

To test the C+L upgrade, SSFM simulations are performed using the framework in [3]. The system has the following characteristics: 10x75 km identical spans of standard single-mode fiber (SSMF), chromatic dispersions of 16.7 ps / (nm · km) and non-linearity coefficients of 1.27 $(W \cdot km)^{-1}$, frequency-dependent fiber loss with an average of 0.18 dB/km, L and C band amplifiers with average noise figures of 4.68 dB and 4.24 dB, respectively. The 64 channels/band utilize PM-16 QAM for transmission, with symbol rates of 64 Gbaud, densely packed within a 75 GHz wavelength-division multiplexing (WDM) grid. The C and L band channels are separated by a guard band of 500 GHz.

The optimization of the channel input power profile is performed as shown in Fig. 3b, where a power offset and tilt to the channel comb in each band is applied to compensate for the tilt induced during propagation. These values are determined from propagation after the first fiber span, and it is assumed that the same launch power profile is recovered at each span by properly setting the EDFA gain and tilt values. The optimal power profile is found by

maximizing and flattening the GSNR of each band and following the approach presented in [5]. The optimization procedure starts by finding the local-optimization, global-optimization (LOGO) power, computed separately for each spectral band with values of $P_{out} = -0.46$ dBm and $P_{out} = -0.62$ dBm per channel for L- and C-bands, respectively. The next stage is to apply the power offset and tilt for each band using the LOGO value as an initial guess. The GSNR delivered by this power configuration is evaluated by employing the generalized GN (GGN) model [6]. The search for the optimal profile takes into account all possible combinations within the problem space of all L- and C-band tilts and offsets are computed.

For each configuration, the average GSNR is evaluated and all profiles within the top 1% are chosen and from these, the profile with the optimal flatness value is selected. The tilt values vary from -0.4 to 0.4 dB/THz with a granularity of 0.1 dB/THz. The power offset values vary from -1.0 to 2.0 dB for the C-band and from -2.0 to 1.0 dB for the L-band, both with a granularity of 0.5 dB. Four different cases are evaluated: (i, ii) the C- and L-bands are optimized independently, (iii) C- and L-bands are jointly optimized, (iv) the C+L transmission is optimized with constrained tilt and offset values for the C-band, retaining the optimum single-band C-only power profile as previously set and investigating the optimum tilt and offset for L-band. The fourth scenario refers to a practical use case where the deployed C-band configuration must not be changed, and the L-band upgrade must be performed while avoiding out-of-service on the deployed C-band lightpaths.
In Fig. 4a, 4b, and 4c are presented the OSNR, SNR_{NL}, and GSNR for all four optimization scenarios analysed. Focusing on the main QoT parameter, which is the GSNR in Fig. 4c, we notice that for C-band systems, the best case is single-band transmission using this band, presenting the highest GSNR average of 20.75. Adding the L-band to this system, the GSNR average decreases, mainly because of the power transfer induced by the SRS. We also notice that joint optimization is the best scenario for a C+L system, with the GSNR decreasing only by an average of 0.25 dB in the C-band, and increasing the L-band average by around 0.25 dB. This increase in L-band GSNR can be explained by the step which was used in the L-band only optimization: due to computational time limitations, the algorithm was not able to find the optimal L-band solution. Finally, maintaining a fixed C-band input power (to simulate an already running system), the degradation in this band, compared with the C-band only scenario, is approximately 0.5 dB, and presents an almost optimal L-band QoT level. Fig. 4d presents a table summarizing the results, with the values of tilt and offset found by the optimization algorithm as well as the GSNR average and variation using those values.

To conclude, the best solution in terms of QoT was found to be the joint C+L optimization. Moreover, when considering an already-operational C-band system, an L-band upgrade can be a viable solution to increase capacity, as it minimally impacts the existing C-band QoT.

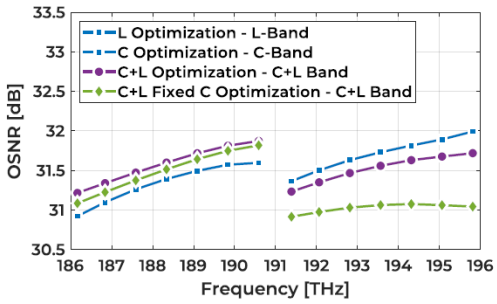

(a)

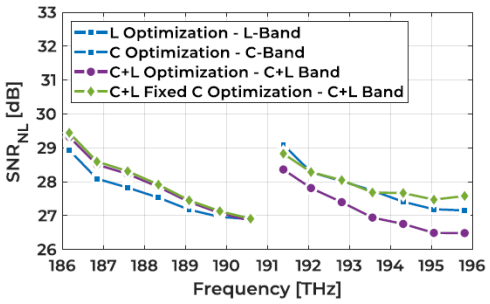

(b)

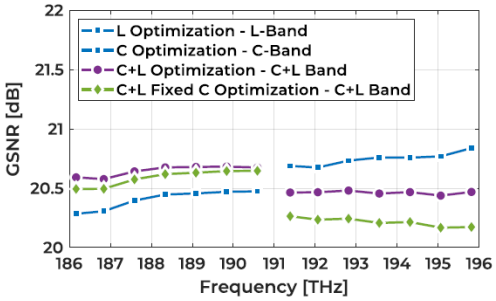

(c)

Optimization	Offset [dB]		Tilt [dB/THz]		Avg. GSNR [dB]		Max. Δ from avg GSNR [dB]	
	L	C	L	C	L	C	L	C
C-only		0.0		0.3		20.75		0.09
L-only	0.0		0.3		20.40		0.12	
Joint C+L	-0.5	0.5	0.4	0.4	20.65	20.46	0.07	0.02
C+L, Fixed C	-0.5	0.0	0.4	0.3	20.59	20.21	0.09	0.05

(d)

Figure 4: The QoT metrics for 10 75 km spans of SSMF OLS, with 7 CUTs per band: (a) OSNR (b) SNR_{NL} (c) GSNR vs channel frequencies. In (d) table reporting the offset (dB difference from the LOGO power) and tilt (dB/THz) values obtained from the input power profile optimization algorithm for single-band (C-only, L-only) and multi-band cases (Joint C+L and the C+L case where the C-band parameters are fixed). For each optimization profile, the average GSNR per band and the maximum deviation from this value are reported.

4. Network performance assessment for C+L+S multi-band optical systems

To evaluate the capacity increases from multi-band solutions (also called band division multiplexing - BDM), we performed a network assessment for three physical topologies, comparing a multi-band implementation with the corresponding spatial division multiplexing (SDM) solution. In this work, the SDM approach represents a multiple-fiber solution, meaning each network link consists of 2, 3, or 4 fibers per link. For all network topologies, the fiber spans in the amplified lines have identical lengths and fiber types of 75 km and ITU-T G.652D SSMF, respectively. Channels within the C- and L-bands utilize commercially available EDFAs, whereas channels located in the S-band are amplified with a Thulium-doped fiber amplifier (TDFA) with characteristics reported in [8]. The noise figure (NF) for the S-band amplifiers is assumed to be 6.5 dB. For C- and L-band amplifiers, the NF average considered is 4.25 and 4.68 dB, respectively. The power optimization used in this assessment is the same as scenario (iv) of Section 3, but considering the addition of the S-band. To set the optimal per-band offset and tilt, a brute-force computation is performed with all combinations analysed and the GSNR evaluated for each scenario by running the GNPy open source project **Error! Reference source not found.**[11]. In this case, a 50 GHz WDM grid is used with 32 Gbaud as symbol rate for four scenarios: (i) C-band only with 96 channels, (ii) C+L with 192 channels, (iii) C+L+S with 288 channels (96 on half of S-band) and (iv) C+L+S with 384 channels (192 channels occupying all S-band). Fig. 5 presents the optimized per-span GSNR profiles for the four multi-band scenarios with tilt and offset values reported in Table 1, obtained via the brute force optimization described with ranges, pre-tilts, and offsets as defined in [13].

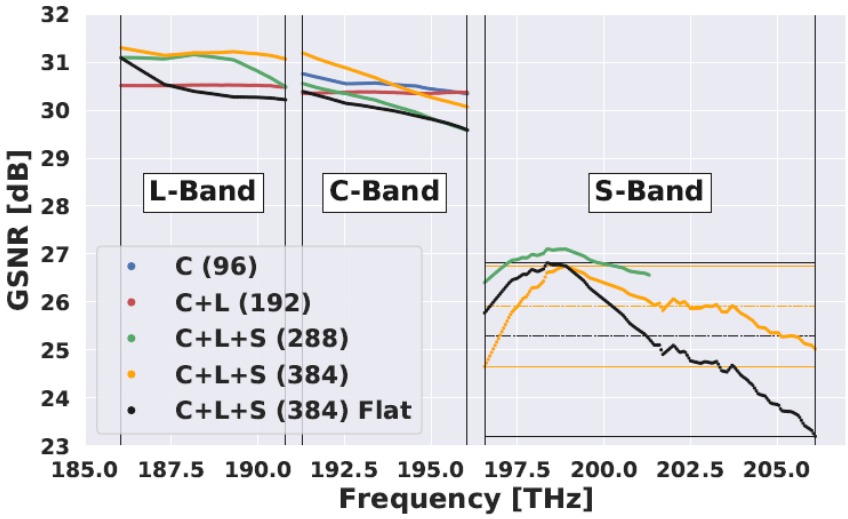

Figure 5: 75 km fiber span GSNR versus frequency for all scenarios, maximum and minimum GSNR for the S-band (lines) and average GSNR (dashed lines) for the S-band, comparing launch power control with flat input powers.

For the C-band-only deployment case (blue curves), the average per-span GSNR in the WDM comb of 96 channels is 30.5 dB. If we activate the L-band with an additional 96 channels (red curves) using a multi-band power controller, the per-span average GSNR is 30.3 dB and 30.5 dB for C- and L-band, respectively. Thus, C+L-band BDM shows a penalty of only 0.2 dB compared to doubling the C-band-only transmission capacity. Even with this decrease, the launch power strategy can deliver an almost flat GSNR profile for both bands. When we activate an additional 96 channels in the S-band, creating a C+L+S-band BDM line system of 288 WDM channels (green curves), the optimal multi-band power control guarantees an average per-span GSNR of 30.1 dB, 31.0 dB, and 26.8 dB for C-, L- and S-

bands, respectively. Within the C+L+S-band BDM implementation, the C-band experiences an additional yet limited average GSNR penalty of 0.2 dB per-span compared to the C+L-band case, while the L-band benefits from SRS pumping into the lowest spectrally located channels, thereby slightly improving its GSNR. The 96 channels on the S-band present a poorer GSNR than the other bands. This is mainly caused by the SRS and by the larger NF of the considered S-band amplifier. As the overall penalty of the S-band is limited to 4 dB, a reasonable transmission capacity is also enabled within this band, along with a limited perturbation on the C+L-band transmission performance. Observing the per-band GSNR flatness, a worse performance than the C+L-band case is shown, but the difference between the maximum and minimum per-band GSNR is confined within 1 dB. Finally, when the entire S-band is activated with 192 channels (orange curves), deploying a C+L+S-band WDM multi-band line system, the optimal multi-band power control ensures an average per-span GSNR of 30.6 dB, 31.2 dB, and 25.9 dB for C-, L- and S-band, respectively.

Table 1: Optimum launch power tilts and offsets per band for the C-, C+L- and both C+L+S-band transmission cases.

Bands (N^0 chann.)	Pre-tilts [dB/THz]			Offsets [dB]		
	L	C	S	L	C	S
C (96)	-	-0.5	-	-	0.0	-
C+L (192)	0.3	0.4	-	-2.0	-1.0	-
C+L+S (288)	-0.5	0.5	0.1	-1.0	-1.0	2.0
C+L+S (384)	-0.5	0.5	0.5	-1.0	-1.0	0.0

Regarding assessing the impact of the different upgrades in an OLS using the GSNR profile found by the power optimization, the allocated traffic with respect to an increasing number of spans numbers is presented in Fig. 6. For 10 spans, the capacity delivered by the C-band only case is 41.2 Tbps with SDM delivering 2, 3, and 4 times more for each scenario tested (82.4, 123.6, and 164.8 Tbps). With the BDM upgrade, also for 10 spans, 82, 117, and 150 Tbps are obtained for all BDM scenarios (192, 288, and 384 channels).

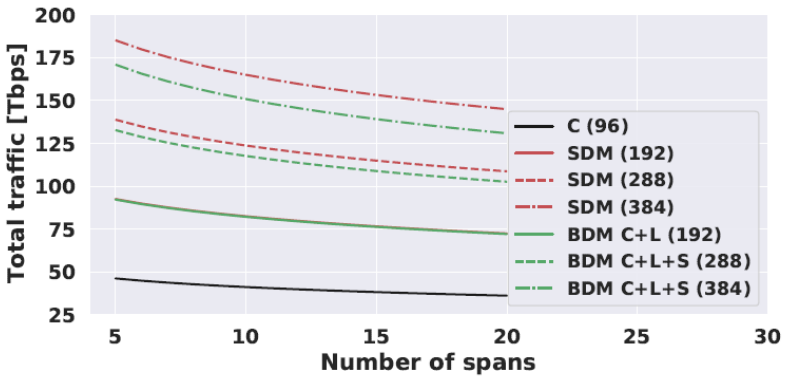

Figure 6: Total allocated traffic vs. number of fiber spans for all upgrade scenarios.

Results of the GSNR optimization are then used as a hypothesis for operational settings in the network control plane, and the network topology can be consequently abstracted for physical-layer-aware networking analyses [13]. The different physical layer optical transport

solutions impact in the network performance is exploited using the statistical network assessment process (SNAP) [14]. SNAP operates based on the GSNR degradation introduced by each network element [13], and statistically tests the network progressive load with different traffic models. Lightpaths are allocated according to the defined routing and wavelength assignment (RWA) algorithm and transceiver characteristics. Networking metrics are obtained statistically by performing Monte Carlo analyses. Three network topologies, shown in Fig. 7, are considered: (i) the German network shown in Fig. 7(a) comprised of 17 optical nodes and 26 edges with an average nodal degree of 3.1, the average distance between nodes of 207 km and maximum link length of 300 km, (ii) the US-NET topology shown in Fig. 7(b) consists of 24 optical nodes and 43 edges, with an average nodal degree of 3.6, the average distance between nodes of 308 km and maximum link length of 525 km, (iii) the European COST network shown in Fig. 7(c) with 28 nodes and 41 edges, an average nodal degree of 2.93, the average distance between nodes of 637 km and maximum link length of 1125 km.

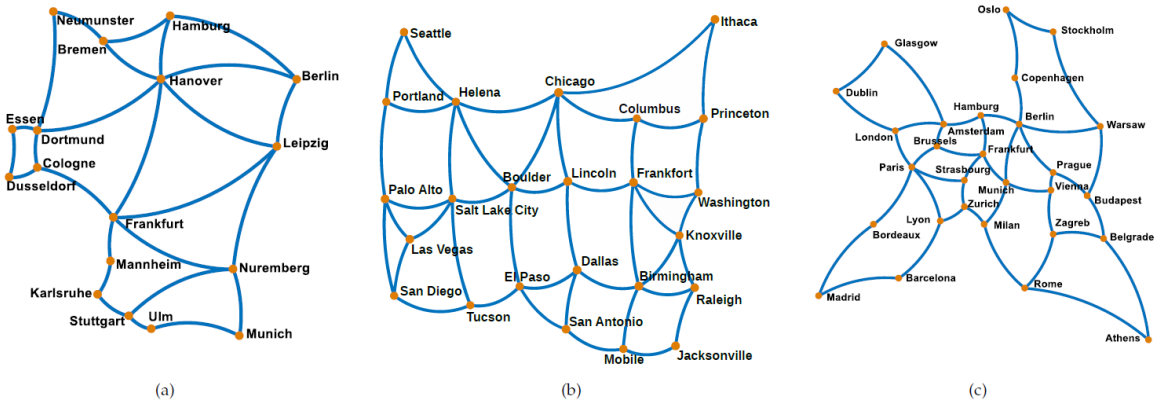

Figure 7: Reference networks analysed: (a) German, (b) US-NET and (c) COST topologies.

To obtain a stable network metric using the SNAP, 3000 iterations are used for the Monte Carlo algorithm in the German topology and 2000 in the US-NET and COST topologies. A *k*-shortest path algorithm is used for routing, with k = 15, and First-Fit (FF) applied for a wavelength assignment (WA) in a progressive traffic analysis to obtain both dynamic and static metrics [14]. Lightpaths requests are progressively generated for each Monte Carlo run, exploring two scenarios with statistical traffic models that are characterized by different JPDFs: a uniform JPDF and distribution based on population [3] as presented in Fig. 8.

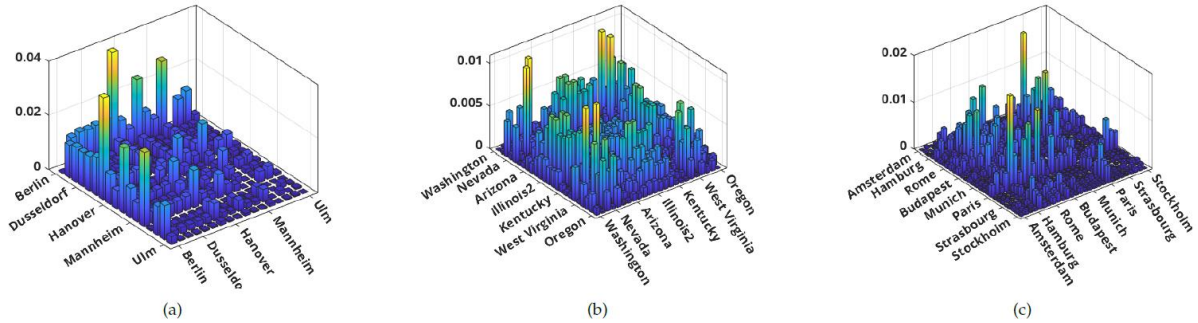

Figure 8: Nonuniform population based JPDF for: (a) German, (b) US-NET and (c) COST topologies.

The network performance is evaluated for the multi-band amplifier power control, with the optimal GSNR profile obtained by the brute force approach. The bit rate over each LP is deployed assuming ideal elastic transceivers that deliver the bit rate according to the available GSNR. For all cases, ROADMs emulate fully loaded OLS's that are able to maintain QoT levels with minimum changes compared to transmitted modulated signals. SNAP is applied to uniform and nonuniform traffic models for the BDM and SDM cases, with the same spectral availability. The following cases are considered: i) the C+L (192) BDM to the SDM 2 x; ii) the C+L+S (288) BDM to the SDM 3x, and finally, iii) the C+L+S-band (384) BDM to the SDM 4x. Results are displayed as a statistical average over the Monte Carlo runs of the BP versus total progressively allocated traffic, for each BDM and equivalent SDM scenario and both traffic models. Taking BP$= 10^{-2}$ as a reference, the traffic values are considered to calculate the enabled traffic multiplication factor, which is used to fairly compare the different transmission solutions. The results are shown in Figs. 9, 10, and 11. In general, for the German network topology of Fig. 9, it seems to be well designed for a traffic model proportional to the population in the urban areas each ROADM node is located, as with a nonuniform traffic model, the deployed total traffic is always larger than for the uniform case. In terms of BDM/SDM upgrade, both solutions enable a traffic multiplication factor always exceeding the BDM/SDM cardinality. Comparing BDM to SDM solutions, the reference SDM scenario outperforms BDM always by less than 3%, confirming that multi-band transmission can be a viable solution to expand network traffic capacity without requiring new fiber infrastructure or utilization of dark fibers. In contrast to the German network topology, the population-based traffic model applied to the US-NET delivered less total traffic than the uniform case, as presented in Fig. 10. For the US-NET, the ROADMS of the most densely populated cities are in the extremes of the topology, demanding ultra-long connections with higher frequency than with the uniform traffic distribution. The multiplicative factor reported in Fig. 10(c) shows that for both upgrade scenarios using BDM can more than double, triple, and quadruple the capacity for the two considered traffic models, with the highest difference in allocated traffic achieving approximately 3.8%, compared with SDM. For the COST topology shown in Fig. 11, the multiplicative factor for both traffic JPDFs follows the behaviour of the previously analysed topologies. The three analysed topologies – with the two traffic models– as shown in Figs. 9, 10 and 11, present the same behaviour of a small increase in the difference of allocated traffic between the BDM and the correspondent SDM technique as we increase the cardinality upgrade. The results are summarized in Table 2, which shows the allocated traffic multiplicative factors for all combinations of topology, upgrade scenario, and traffic JPDF.

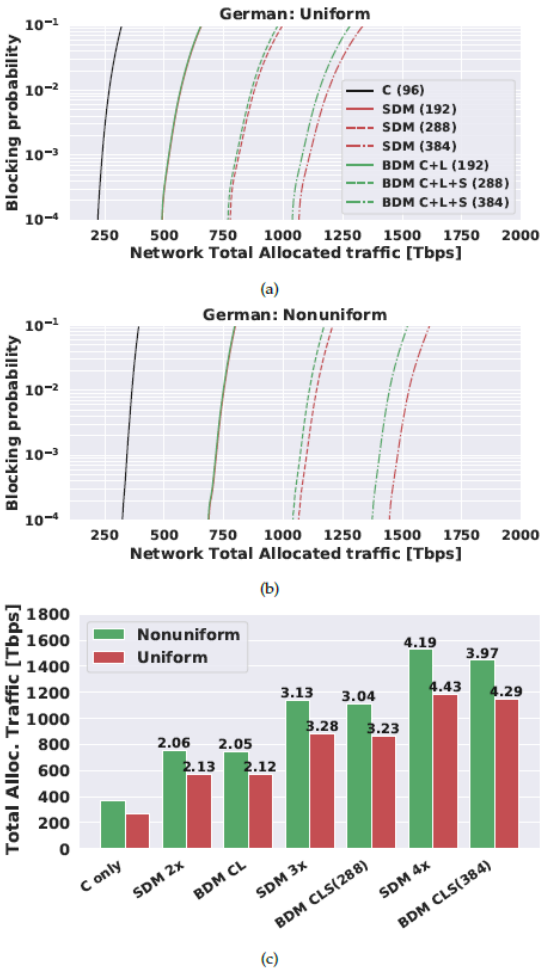

Figure 9: Network performance results for German topology: Total allocated traffic versus BP with (a) Uniform and (b) Nonuniform JPDFs, and (c) total allocated traffic multiplicative factor for BP$= 10^{-2}$.

Table 2: Allocated traffic multiplicative factors (C-only as reference) of German, US-NET and COST topologies for all upgrade scenarios and traffic distributions with BP$= 10^{-2}$.

Topology	German		US-NET		COST	
Upgrade	Uniform	Nonuniform	Uniform	Nonuniform	Uniform	Nonuniform
SDM 2×	2.13	2.06	2.04	2.06	2.1	2.05
C+L	2.12	2.05	2.03	2.05	2.09	2.04
SDM 3×	3.28	3.13	3.09	3.1	3.21	3.09
C+L+S (288)	3.23	3.04	3.03	3.05	3.13	3.02
SDM 4×	4.43	4.19	4.14	4.16	4.34	4.13
C+L+S (384)	4.29	3.97	3.97	4.0	4.11	3.93

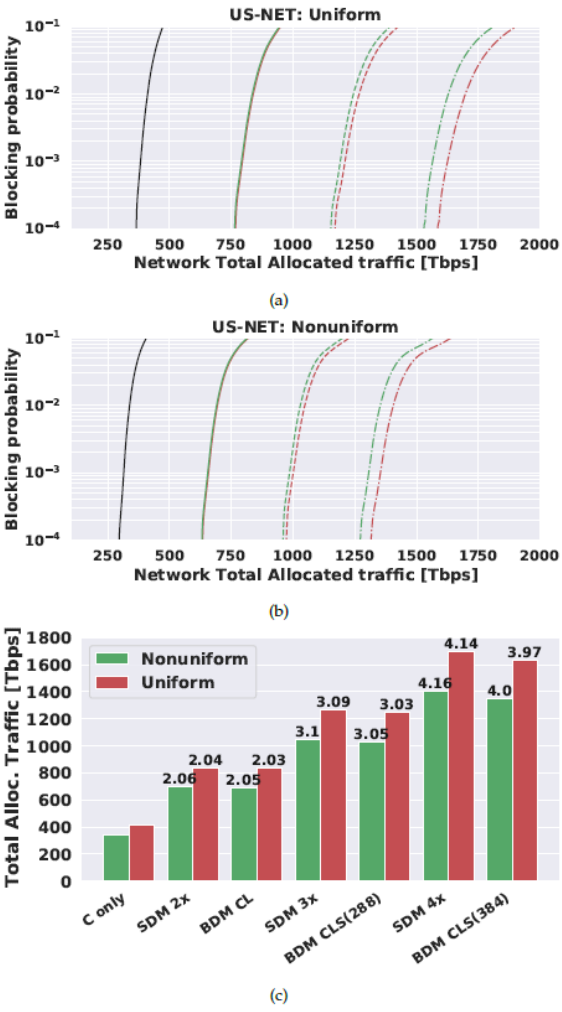

Figure 10: Network performance results for US-NET topology: Total allocated traffic versus BP with (a) Uniform and (b) Non-uniform JPDFs, and (c) total allocated traffic multiplicative factors for BP$= 10^{-2}$.

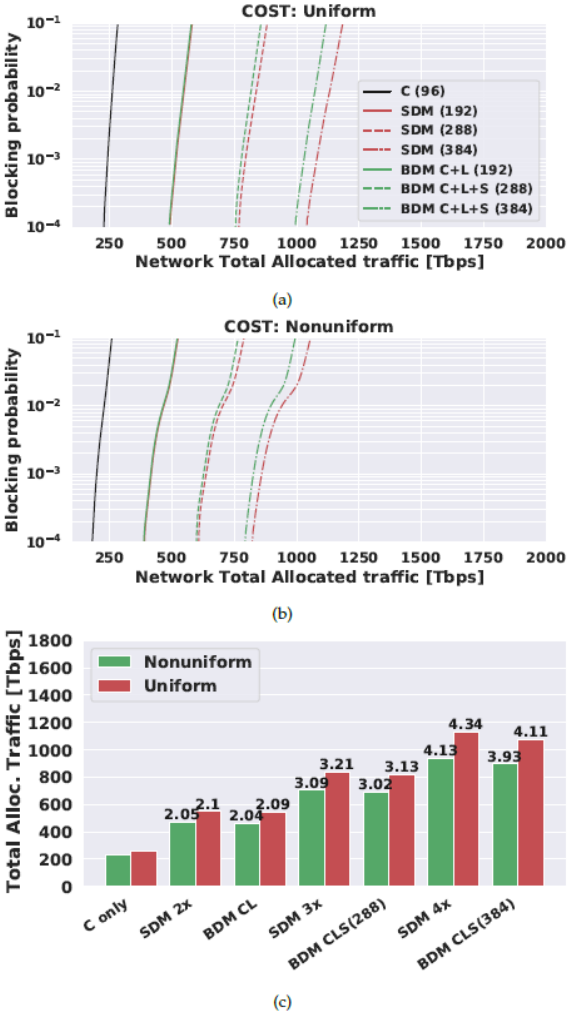

Figure 11: Network performance results for COST topology: Total allocated traffic versus BP with (a) Uniform and (b) Nonuniform JPDFs, and (c) total allocated traffic multiplicative factor for BP$= 10^{-2}$.

5. CONCLUSIONS

In this work, we present the results of a simulation campaign where the NLI is considered from a disaggregated approach, where the XPM and SPM contributions are managed in a fully spectrally and spatially separated approach. We show a power control management benchmark for use in multiband systems, considering the C, L, and S-bands. Some major points can be highlighted: (i) when the history of a lightpath is unknown, the GN-model always provides a worst-case NLI prediction. (ii) upgrading a C-band OLS consisting of 10 x 75 km spans of SSMF to C+L-band transmission is feasible with a minimal average GSNR penalty of only 0.25 dB in the C-band for a joint multi-band power control scenario. (iii) BDM solutions generally enable a large traffic upgrade with a multiplication factor that does not exceed the upgrade cardinality.

It is important to highlight that the results and approaches presented in this deliverable are summaries that contain only a subset of obtained results. Additional details can be found in other recent publications by the project contributors [13],**Error! Reference source not found.** [16], [17] and a preceding work [18] which explain these conclusions in greater detail.

6. REFERENCES

[1] Cisco Visual Networking Index: Forecast and Methodology, 2018, [Online].

[2] Filer, Mark, et al. "Multi-vendor experimental validation of an open source QoT estimator for optical networks." Journal of Lightwave Technology 36.15 (2018): 3073-3082.

[3] Virgillito, Emanuele, et al. "Network performance assessment of C+ L upgrades vs. fiber doubling SDM solutions." Optical Fiber Communication Conference. Optical Society of America, 2020.

[4] D. Pilori, et al. FFSS: The fast fiber simulator software. ICTON, pages 1–4. IEEE, 2017.

[5] Virgillito, Emanuele, et al. "Network performance assessment with uniform and non-uniform nodes distribution in C+ L upgrades vs. fiber doubling SDM solutions." 2020 International Conference on Optical Network Design and Modeling (ONDM). IEEE, 2020.

[6] Pastorelli, R., et al. "Optical control plane based on an analytical model of non-linear transmission effects in a self-optimized network." 39th European Conference and Exhibition on Optical Communication (ECOC 2013). IET, 2013.

[7] Pilori, Dario, et al. "Observing the effect of polarization mode dispersion on nonlinear interference generation in wide-band optical links." OSA Continuum 2.10 (2019): 2856-2863.

[8] "Amp-fl8221-sb-16 amplifier datasheet from fiber labs inc".

[9] V. Curri, A. Carena, A. Arduino, G. Bosco, P. Poggiolini, A. Nespola, and F. Forghieri, "Design strategies and merit of system parameters for uniform uncompensated links supporting Nyquist WDM transmission," J. Light. Technol. 33, 3921–3932 (2015).

[10] Poggiolini, Pierluigi, et al. "The LOGON strategy for low-complexity control plane implementation in new-generation flexible networks." 2013 Optical Fiber Communication Conference and Exposition and the National Fiber Optic Engineers Conference (OFC/NFOEC). IEEE, 2013.

[11] Ferrari, Alessio, et al. "GNPy: an open source application for physical layer aware open optical networks." Journal of Optical Communications and Networking 12.6 (2020): C31-C40.

[12] "GitHub repository of GNPy," https://github.com/Telecominfraproject/oopt-gnpy.

[13] Correia, Bruno, et al. "Power control strategies and network performance assessment for C+ L+ S multiband optical transport." Journal of Optical Communications and Networking 13.7 (2021): 147-157.

[14] Curri, Vittorio. "Software-defined WDM optical transport in disaggregated open optical networks." 2020 22nd International Conference on Transparent Optical Networks (ICTON). IEEE, 2020.

[15] Curri, Vittorio, Mattia Cantono, and Roberto Gaudino. "Elastic all-optical networks: A new paradigm enabled by the physical layer. how to optimize network performances?." Journal of Lightwave Technology 35.6 (2017): 1211-1221.

[16] London, Elliot, et al. "Observing cross-channel NLI generation in disaggregated optical line systems." 2022 Optical Fiber Communications Conference and Exhibition (OFC). IEEE, 2022 (submitted).

[17] Virgillito, Emanuele, et al. "Single-vs. Multi-Band Optimized Power Control in C+ L WDM 400G Line Systems." 2021 Optical Fiber Communications Conference and Exhibition (OFC). IEEE, 2021.

[18] London, Elliot, et al. "Simulative assessment of non-linear interference generation within disaggregated optical line systems." OSA Continuum 3.12 (2020): 3378-3389.